Transverse flow and hadrochemistry in Au+Au collisions at $\sqrt{s_{NN}}=200$ GeV

Peter F. Kolb[1] and Ralf Rapp[2]
[1]*Department of Physics and Astronomy, SUNY, Stony Brook, New York 11794-3800*
[2]*NORDITA, Blegdamsvej 17, DK-2100 Copenhagen Ø, Denmark*
(Received 17 October 2002; published 24 April 2003)

We present a hydrodynamic assessment of preliminary particle spectra observed in Au+Au collisions at $\sqrt{s_{NN}}=200$ GeV. The hadronic part of the underlying equation of state is based on explicit conservation of (measured) particle ratios throughout the resonance gas stage after chemical freezeout by employing chemical potentials for stable mesons, nucleons, and antinucleons. We find that under these conditions the data (in particular, the proton spectra) favor a low freezeout temperature of around ~100 MeV. Furthermore, we show that through inclusion of a moderate prehydrodynamic transverse flow field the shape of the spectra improves with respect to the data. The effect of the initial transverse boost on elliptic flow and the freezeout geometry of the system is also discussed.

DOI: 10.1103/PhysRevC.67.044903 PACS number(s): 25.75.Dw, 25.75.Ld, 24.10.Nz

I. INTRODUCTION

During its second year of operation, RHIC (the relativistic heavy ion collider at Brookhaven National Laboratory) has collided ^{197}Au nuclei at center-of-mass (c.m.) energies of 200 GeV per nucleon pair to create strong interaction matter at high-energy densities in the laboratory. To identify signals of a possible phase transition from low-energy nuclear to deconfined quark-gluon matter, a large amount of data was analyzed and recently presented for the first time [1].

In the present paper we investigate single-particle spectra of various hadronic species within a hydrodynamic framework for the reaction dynamics, which assumes rapid thermalization in the reaction volume and a subsequent expansion according to the conservation of energy, momentum, entropy, and baryon number (for details of the approach, which resides on explicit longitudinal boost invariance, cf. Ref. [2]). At c.m. energies of 130*A* GeV, the successful description of observed single-particle transverse momentum (p_{T}) spectra and their azimuthal modulation in noncentral collisions have validated this approach down to decoupling temperatures of ~130 MeV, at which hadronic interactions have been assumed to cease instantaneously [3]. As an alternative to entirely hydrodynamic simulations, especially for the late, more dilute stages in a heavy-ion collision, hybrid models have been developed [4–6], which treat the hadronic phase in sequential-scattering models, propagating hadrons individually. While the momentum-space observables are in good agreement with experiments at RHIC in both descriptions, the freezeout geometry persists to be inconsistent with the data in either approach. Hydrodynamic evolutions appear to be too long-lived but too small in radial extent [7], whereas hybrid calculations produce an emission cloud that appears to be too large [4,5].

Concerning global particle production, it was soon realized [8] that, also at RHIC energies, measured hadron ratios reflect a chemical composition of the fireball that corresponds to a temperature close to the expected QCD phase boundary, $T_{chem}\simeq 170$–180 MeV$\simeq T_c$. Thus, in a thermodynamic description of the cooling process from chemical to thermal freezeout, the conservation of the relative hadronic abundances requires the introduction of (effective) chemical potentials [9–14] for species that are stable on the scale of typical fireball lifetimes. In particular, it was pointed out in Ref. [13] that the conservation of antibaryons plays an important role at collider energies. Despite their large annihilation cross sections, their finally observed abundance is in complete agreement with chemical-freezeout systematics (for a possible microscopic explanation of this fact, based on multimeson fusion reactions to maintain detailed balance, cf. Ref. [15]). This implies the buildup of large antibaryon chemical potentials, $\mu_{\bar{\mathrm{N}}}^{\mathrm{eff}}$, defined via $\mu_{\bar{\mathrm{N}}}=-\mu_{\mathrm{N}}+\mu_{\bar{\mathrm{N}}}^{\mathrm{eff}}$. Towards thermal freezeout this, in turn, entails rather large baryon chemical potentials ($\mu_N\simeq 350$ MeV), and is at the origin of appreciable pion chemical potentials ($\mu_\pi \simeq 80$–100 MeV). The influence of chemical potentials on the hydrodynamic evolution and resulting observables has been investigated in Ref. [16] for c.m. energies of 130*A* GeV. In addition to conserving π, K, η, and η' numbers, we here explicitly distinguish chemical potentials of baryons and antibaryons along the lines of Ref. [13] to correctly account for the finite net-baryon density at full RHIC energy (200*A* GeV). For consistency with previous analyses [2,3,17,18] we assume a phase transition from quark gluon to hadron matter at $T_c=165$ MeV with a latent heat of $e_{\mathrm{lat}}=1.15$ GeV/fm^3 and a hadronic resonance gas equation of state (EoS) as before. At T_c the hadronic phase starts in chemical equilibrium to (approximately) reproduce the measured particle ratios [8], see above. To improve on previous analyses, the subsequent hadronic evolution is now constructed incorporating effective meson and (anti)baryon chemical potentials as in Ref. [13] to preserve the correct (absolute) particle abundances.

As a second new aspect of the present manuscript, we present an attempt to refine the initial conditions of the hydrodynamic evolution. More specifically, we will explore ramifications of preequilibrium collective behavior by introducing appropriate radial velocity profiles at the time of complete thermalization. Such effects can be associated with prethermal reinteractions, a free-streaming period, or a combination thereof, and turn out to generally improve the de-

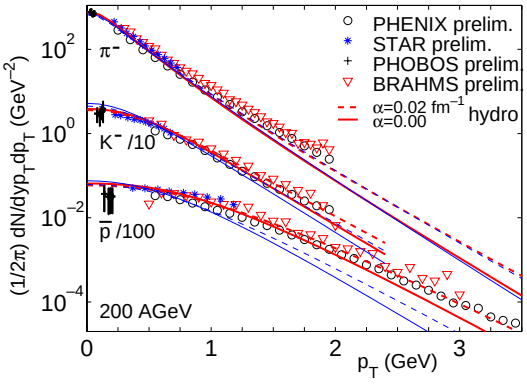

FIG. 1. π^-, K^-, and antiproton spectra for central collisions at 200*A* GeV (K^- and $\bar{p}$ spectra are scaled by factors of 1/10 and 1/100, respectively). The thick lines represent the results for $T_{\rm dec}=100$ MeV, the thin lines for 165 MeV. All calculations are for a thermalization time $\tau_0=0.6$ fm/c, either *without* (solid lines) or *with* (dashed lines) an initial transverse boost (see text).

scription of transverse momentum spectra of the produced particles.

Our paper is organized as follows. In Secs. II and III we analyze the impact (and interplay) of off-equilibrium hadrochemistry and modified initial collisions on transverse momentum spectra of pions, kaons, and (anti) protons, both for central and more peripheral collisions in comparison to preliminary data at 200*A* GeV. Pertinent predictions for azimuthal anisotropies in noncentral collisions are presented in Sec. IV. We furthermore comment on implications for the freezeout geometry in Sec. V, and summarize in Sec. VI.

II. PARTICLE SPECTRA—CENTRAL COLLISIONS

Let us start by briefly discussing the initial conditions of our hydrodynamic calculations. According to the $\sim$15% larger hadron multiplicity at midrapidity in central collisions at 200*A* GeV [19,20] as compared to 130*A* GeV, we increase the maximum entropy-density parameter from $s_0=95$ fm^{-3} [7] to 110 fm^{-3} (keeping the equilibration time fixed at $\tau_0=0.6$ fm/c to facilitate the interpretation of observed changes). The correct baryon admixture is obtained by adjusting the entropy per baryon to $S/B=s_0/n_0=250$, constant throughout the evolution (s_0 and n_0 are the initial entropy density and baryon density in the center of the collision and S and B are the total entropy and net baryon number). The thermodynamic fields in the transverse plane are set to scale with a combination of wounded nucleon and binary collision profiles as elaborated in Refs. [7,18], which allows for a geometrical prescription to reproduce the multiplicity in collisions at finite impact parameter b.

The results of our calculations with improved hadrochemistry are compared to (preliminary) data for π^-, K^-, and antiproton $p_{\rm T}$ spectra from central Au+Au collisions at 200*A* GeV [21,22] in Fig. 1 (the experimental centrality selection of 5% is approximated by using an average impact parameter $b=2.4$ fm). Compared to particle spectra in standard i.e., chemical-equilibrium) hydrodynamics, we find a better description of the overall curved shape of the hadronic spectra, in particular, for low-$p_{\rm T}$ pions. This is a result of the meson chemical potentials ($\mu_\pi\approx 80-100$ MeV at freezeout), which amplify the Bose-statistics effect. In addition, the population of heavy resonances also increases after inclusion of chemical potentials, which entails larger contributions at low $p_{\rm T}$ from their decay products. At large transverse momenta the hydrodynamic calculations deviate from the data which is suggestive for the onset of the hard scattering regime. At exactly which values of $p_{\rm T}$ this occurs, and how this transition depends on the particle species, are among the major questions to be clarified. For example, high-energy partons evolving within a hydrodynamic background can be introduced to study the particle spectra beyond the collective behavior [23].

As was already observed in Ref. [16], the expansion of the chemically nonequilibrated hadron gas leads to slopes for pion spectra that are almost insensitive to the decoupling temperature. Proton spectra, on the contrary, clearly favor a freezeout at $T\simeq 100$ MeV (thick solid line), which corresponds to an energy density $e\simeq 0.075$ GeV/fm^3 (which is about the same as in previous calculations). The thin lines in Fig. 1 correspond to decoupling at the phase transition (recall that the multiplicity of the individual particle species is independent of freezeout due to the chemical potentials).

The experimental pion spectra in the 1–2 GeV range appear flatter than what follows from the flow generated by hydrodynamic expansion with our given initial configuration (at transverse momenta $p_{\rm T}\geqslant 2$ GeV this is conceivably due to additional perturbative hard scattering contributions). To a lesser extent, this is also true for the heavier kaons and protons, even at the low freezeout temperature of 100 MeV.

The data thus seem to exhibit somewhat stronger collective expansion than developed subsequent to an equilibration time of $\tau_0=0.6$ fm/c. Additional radial flow could be generated by assuming still shorter equilibration times, e.g., $\tau_0=0.2$ fm/c [24]. It is, however, hard to imagine that particles are "born" into thermal equilibrium without allowing for some relaxation time with rescattering. But even the other extreme, i.e., a period of free streaming, induces a nonvanishing radial velocity profile due to a separation of originally random particle velocities [25,7]. A realistic situation is probably in between the two extremes, essentially preequilibrium in character with associated rather complicated structures of the generated flow-field and energy-density distributions (more exotic phenomena such as sphaleron explosions [26] could also play a role). As an exploratory study, we here introduce a simplistic initial "seed" transverse velocity according to $v_{\rm T}(r)=\tanh(\alpha r)$, where r is the radial distance from the origin, superimposed on the original fields at $\tau_0=0.6$ fm/c. For a value of $\alpha=0.02$ fm^{-1} the initial velocity field for $r_\perp\leqslant 6$ fm/c is similar in magnitude (although less parabolic) to both (i) starting the hydrodynamic evolution at earlier time ($\tau_0=0.2$ fm/c as in Ref. [24]) and evolving it to $\tau_0=0.6$ fm/c, as well as (ii) free streaming from $\tau=0.2$ to 0.6 fm/c. The essential difference between (i) and (ii) lies in the azimuthal distribution at $\tau_0=0.6$ fm/c, to which we will come back to in Sec. IV. It should also be noted that stronger transverse flow due to larger transverse pressure is expected if the longitudinal expansion is not fully thermalized [27].

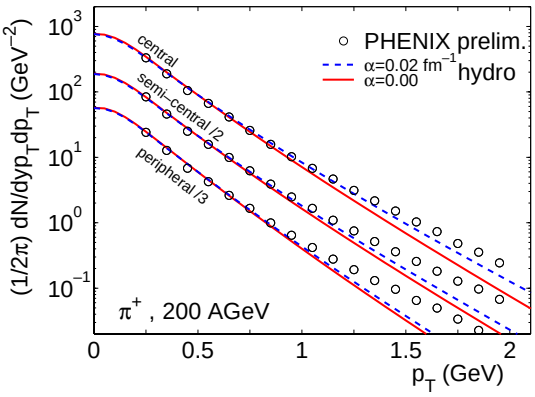

FIG. 2. Centrality dependence of positive pion spectra at midrapidity ($y=0$) in terms of central, semicentral (scaled by 1/2), and peripheral collisions (scaled by 1/3).

The results with our simple ansatz are represented by the dashed lines in Fig. 1, and are found to improve the agreement with experiment, up to $p_T \simeq 2(3.5)$ GeV for pions and kaons (antiprotons). We note that when increasing α to 0.05, the proton spectra become much flatter than experimentally observed.

III. PARTICLE SPECTRA—NONCENTRAL COLLISIONS

In Fig. 2 we compare preliminary spectra of positive pions [21] to our hydrodynamic results at $T_{dec}=100$ MeV in three different centrality bins ("central," $b=2.4$ fm, $N_{part}=343.8$; "semicentral," $b=7$ fm, $N_{part}=170.8$; "peripheral," $b=9.6$ fm, $N_{part}=76.6$). Again, we display calculations with an initial transverse boost by dashed lines. As expected, the prerequisites for a hydrodynamic approach (strong rescattering and a sufficiently large system size) are increasingly invalidated at large impact parameters, reflected by an onset of deviations from experiment at smaller transverse momenta (higher-momentum particles can rapidly escape the fireball without thermalizing). For peripheral collisions the agreement between theory and experiment holds for $p_T \leqslant 1$ GeV, which, nevertheless, still accounts for more than 96% of the emitted particles.

Figure 3 shows experimental [21] and calculated proton

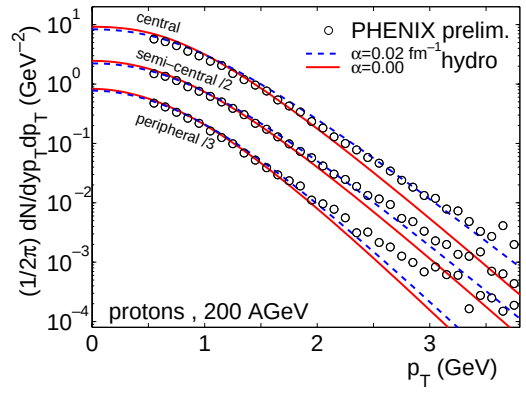

FIG. 3. Midrapidity proton spectra for central, semicentral (scaled by 1/2), and peripheral collisions (scaled by 1/3).

TABLE I. Multiplicities and mean transverse momenta (in GeV) of different particles for three centrality selections (1=central, 2=semicentral, 3=peripheral) at $y=0$. The $\bar{p}/p$ ratio is 0.72; $\langle p_T \rangle$ of antiprotons is within 1% of the proton value.

		$\alpha=0.00$			$\alpha=0.02$ fm^{-1}		
		1	2	3	1	2	3
π^+	$\frac{dN}{dy}$	280.8	134.3	57.84	282.3	134.6	57.82
	$\langle p_T \rangle$	0.398	0.392	0.375	0.419	0.405	0.383
K^+	$\frac{dN}{dy}$	50.18	23.99	10.33	50.43	24.05	10.33
	$\langle p_T \rangle$	0.619	0.608	0.572	0.660	0.634	0.589
p	$\frac{dN}{dy}$	28.08	13.44	5.798	28.13	13.44	5.794
	$\langle p_T \rangle$	0.880	0.861	0.802	0.949	0.906	0.831

spectra, which are of particular interest in the present context as they acquire the largest chemical potentials (e.g., around thermal freezeout $\mu_N=380$ MeV and $\mu_{\bar{N}}=343$ MeV implying $\mu_{\bar{N}}^{eff}=723$ MeV, which yields an antiproton-to-proton ratio of 0.72 consistent with experiment [28]), and are most sensitive to collective expansion. We find good agreement of theory and experiment at a freezeout temperature of 100 MeV up to $p_T \simeq 3.5$ GeV in the central sample, but only up to ~ 2 GeV in the peripheral sample. The additional transverse "kick" in the initial state as described above (dashed lines) is particularly significant for central collisions.

Despite the fact that particle densities in the later hadronic stage of the expansion are moderate, we conclude that rescattering is strong enough to allow for a hydrodynamic description until thermal decoupling. The correct chemical composition of the hadronic gas is maintained by the generation of large chemical potentials, which (at given temperature) provide an increased number of scattering partners with larger cross sections as compared to a chemically equilibrated environment.

We have focused here on positively charged pions and protons. The corresponding results for π^-, K^+, K^-, and $\bar{p}$ in noncentral collisions are of similar quality. The multiplicities and mean transverse momenta of these particles are collected in Table I.

IV. ELLIPTIC FLOW

For the same impact parameters as considered above, we proceed by studying the azimuthal anisotropies of particle spectra [29], i.e., the momentum dependence of elliptic flow as defined by $v_2(p_T;b)=\langle \cos(2\phi) \rangle$, where the average is taken over the angular distribution of particles, $dN/dy p_T dp_T d\phi$.

Flow anisotropy is generated during the earliest stages of the collision, at which the spatial eccentricity of the thermodynamic fields and the anisotropies in the pressure gradients

are the largest. The matter is set into anisotropic motion as larger forces are acting along the ''short'' radius of the initial (overlap) ellipse. This motion rapidly reduces the spatial anisotropies, thereby bringing further generation of momentum anisotropy (i.e., v_2) to a stall [30,2]. If the system evolves in chemical equilibrium, the dominant particle species at freezeout are pions, which carry the generated anisotropy in their momentum distribution. Their differential elliptic flow $v_2(p_T)$ is then almost independent of the decoupling temperature T_{dec} [3]. Heavier particles, on the other hand, do exhibit some dependence on T_{dec}, mainly because of the continuously increasing radial flow that shifts the generated anisotropy towards larger transverse momenta. In the presence of effective chemical potentials the contribution of protons to the *total* anisotropic flow (of all particles) is still small; however, the contribution of their number to the particle yield is more significant. The anisotropic flow must thus be absorbed by the pions (which, due to their small masses, adjust their momentum distribution easily). Through this effect their elliptic flow now also becomes sensitive to the decoupling temperature, as found in Ref. [16]. In addition, the influence of resonance decays is enhanced in the chemical off-equilibrium formulation. The heavy resonances, which at large transverse momentum carry rather large elliptic flow, decay and transfer their elliptic flow to pions at relatively low transverse momentum.

In Fig. 4 we show results for elliptic flow of pions (left panel) and protons (right panel) from the hydrodynamic calculation under inclusion of chemical potentials. The initial transverse boost as defined in Sec. II shifts the anisotropy to larger transverse momenta, which implies a reduction of v_2 at given p_T. The development of anisotropic flow is additionally hindered since it has to form on top of the *isotropic* initial boost field employed here. The value ϵ_p at which the anisotropy of the energy-momentum tensor of the fluid $T^{\mu\nu}$ saturates during the evolution [2] is about 25% smaller than without the initial kick.

It is instructive to compare these results to the scenario where the equilibration time is set to very small values ($\tau_0 = 0.2$ fm/c for the dashed-dotted curves in Fig. 4). As elucidated in Sec. II, this generates as much *radial* flow as the superimposed profile at $\tau_0 = 0.6$ fm/c does. However, the elliptic flow is larger than in the former case, but *not* significantly different from using an equilibration time of 0.6 fm/c *without* initial kick. This is due to the fact that, without the initial kick, v_2 saturates for either equilibration time at approximately the same value.[1]

The experimentally observed elliptic flow reaches a limiting maximal value as a function of transverse momentum. The PHENIX collaboration has pointed out [21] that this saturation is reached at smaller transverse momenta for pions than for protons, and that the saturation value appears to be larger for the latter. Within the hydrodynamic framework this reflects the earlier breakdown of the strong rescattering assumption for pions, which for protons remains valid up to higher p_T due to larger (average) scattering cross sections ($\sigma_{\pi N} > \sigma_{\pi\pi}$). This is corroborated by the description of the single-particle spectra that extends to larger p_T for (anti)protons than for pions. The different v_2-saturation momenta for mesonic and baryonic elliptic flow are also consistent with the formation of hadrons via quark coalescence [31]. Within this picture, one similarly expects a larger saturation value of v_2 for protons than for pions.

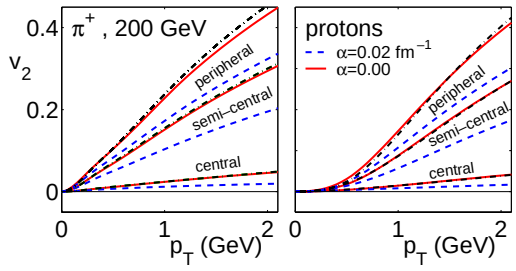

FIG. 4. Elliptic flow of positively charged pions (left) and protons (right) for three different impact parameters. The dashed lines include an initial transverse boost as described in the text. Dashed-dotted lines represent the results when assuming thermalization at $\tau_0 = 0.2$ fm/c with $\alpha = 0$.

V. FREEZEOUT GEOMETRY

Let us finally comment on the implications of our results for the freezeout geometry of the hadronic system. In Ref. [14] it was pointed out that the relation between energy density and pressure, $e(p)$, for the hadronic equation of state is barely modified by the introduction of chemical potentials. Therefore, the space-time evolution of the system, which is largely driven by this relation, is not substantially altered either. A large change, however, occurs in the relation between temperature and energy density, $T(e)$, which thus influences the construction of the freezeout hypersurface and the thermal properties of the fluid on this surface. For example, in chemical equilibrium, the energy density at $T = 130$ MeV corresponds to a temperature of only 100 MeV in the presence of large chemical potentials, since the latter increase particle and energy densities approximately by pertinent fugacity factors $e^{\mu/T}$. Therefore, the freezeout hypersurface of the hydrodynamic calculations in chemical off-equilibrium is not much different from the hypersurface of previous calculations if freezeout is performed at a comparable energy density (i.e., the freezeout temperature is adapted accordingly). In both cases, the fireball decouples at about 15 fm/c after equilibration (in central collisions) and has about the same spatial extent. Only after inclusion of the initial radial flow profile is the lifetime shortened by $\sim 15\%$, and the transverse expansion increases by about the same percentage. For observables, this entails smaller longitudinal correlation radii (which reflect the system's lifetime) but only slightly larger sideward radii. This effect reduces the discrepancies between calculated and measured Hanbury Brown and Twiss (HBT) radii by a few percent [7], but is not sufficient by itself. Additional effects, such as viscosity [32],

[1]Note that this is no longer true for significantly larger τ_0, e.g., 2 fm/c, for which v_2 is significantly reduced and underpredicts the data already at 130*A* GeV.

large partonic cross sections in the early phases [33], or a refined treatment of hadronic rescattering [5] and freezeout [34] (including, e.g., a large ρ-meson width as predicted in Ref. [35]), seem to be required to fully resolve the ''HBT puzzle.''

VI. SUMMARY

Based on a resonance gas equation of state that explicitly incorporates hadrochemical freezeout by employing chemical potentials for (stable) mesons and baryons in the hadronic evolution, we have performed hydrodynamic simulations of heavy ion collisions at full RHIC energy. We have compared the results for pion, kaon, and proton p_T spectra to preliminary data from 200*A* GeV Au+Au collisions at different centralities. Our investigations indicate the necessity of an initial (prehydrodynamic) transverse flow to better account for the slopes of the observed spectra. Good agreement with preliminary data for transverse momentum spectra in central collisions is obtained up to $\sim$1.5–2 GeV for pions, and up to at least 3 GeV for protons. We further studied the influence of hadrochemistry and initial flow on elliptic flow and source geometry. The former has been presented as a prediction for pions and protons for upcoming experimental analyses. For the latter, some improvement with respect to the discrepancy between model and data has been found, but additional effects remain mandatory.

ACKNOWLEDGMENTS

We thank U. Heinz and E. V. Shuryak for fruitful discussions and critical remarks on the manuscript. This work was supported in part by the U.S. Department of Energy under Grant No. DE-FG02-88ER40388. P.F.K. acknowledges support from the Alexander von Humboldt Foundation.

[1] *Proceedings of the 16th International Conference on Ultra-Relativistic Nucleus-Nucleus Collisions, Quark Matter 2002* [Nucl. Phys. **A715**, 1 (2003).]
[2] P.F. Kolb, J. Sollfrank, and U. Heinz, Phys. Rev. C **62**, 054909 (2000).
[3] P.F. Kolb, P. Huovinen, U. Heinz, and H. Heiselberg, Phys. Lett. B **500**, 232 (2001); P. Huovinen, P.F. Kolb, U. Heinz, P.V. Ruuskanen, and S.A. Voloshin, *ibid.*, **503**, 58 (2001).
[4] S.A. Bass and A. Dumitru, Phys. Rev. C **61**, 064909 (2000).
[5] S. Soff, S.A. Bass, and A. Dumitru, Phys. Rev. Lett. **86**, 3981 (2001).
[6] D. Teaney, J. Lauret, and E.V. Shuryak, Phys. Rev. Lett. **86**, 4783 (2001).
[7] U. Heinz and P.F. Kolb, Nucl. Phys. **A702**, 269 (2002).
[8] P. Braun-Munzinger, D. Magestro, K. Redlich, and J. Stachel, Phys. Lett. B **518**, 41 (2001).
[9] M. Kataja and P.V. Ruuskanen, Phys. Lett. B **243**, 181 (1990).
[10] H. Bebie, P. Gerber, J.L. Goity, and H. Leutwyler, Nucl. Phys. **B378**, 95 (1992).
[11] C.M. Hung and E. Shuryak, Phys. Rev. C **57**, 1891 (1998).
[12] N. Arbex, F. Grassi, Y. Hama, and O. Socolowski, Jr., Phys. Rev. C **64**, 064906 (2001).
[13] R. Rapp, Phys. Rev. C **66**, 017901 (2002).
[14] D. Teaney, nucl-th/0204023.
[15] R. Rapp and E.V. Shuryak, Phys. Rev. Lett. **86**, 2980 (2001).
[16] T. Hirano and K. Tsuda, Phys. Rev. C **66**, 054905 (2002).
[17] P.F. Kolb, J. Sollfrank, and U. Heinz, Phys. Lett. B **459**, 667 (1999).
[18] P.F. Kolb, U. Heinz, P. Huovinen, K.J. Eskola, and K. Tuominen, Nucl. Phys. **A696**, 197 (2001).
[19] B.B. Back *et al.*, PHOBOS Collaboration, Phys. Rev. Lett. **88**, 022302 (2002).
[20] I.G. Bearden *et al.*, BRAHMS Collaboration, Phys. Rev. Lett. **88**, 202301 (2002).
[21] T. Chujo for the PHENIX Collaboration, nucl-ex/0209027 (to be published in Ref. [1]); J. Burward-Hoy for the PHENIX Collaboration, nucl-ex/0210001 (to be published in Ref. [1]).
[22] O. Barannikova and F. Wang for the STAR Collaboration, nucl-ex/0210034; B. Wosiek for the PHOBOS Collaboration, nucl-ex/0210037; D. Ouerdane for the BRAHMS Collaboration, nucl-ex/0212001; P. Christiansen for the BRAHMS Collaboration, nucl-ex/0212002; (all contributions to be published in Ref. [1]).
[23] T. Hirano and Y. Nara, Phys. Rev. C **66**, 041901(R) (2002).
[24] K.J. Eskola, H. Niemi, P.V. Ruuskanen, and S.S. Räsänen, hep-ph/0206230.
[25] P. F. Kolb, Ph.D. thesis, Universität Regensburg, 2002, available at http://www.bibliothek.uni-regensburg.de/opus/volltexte/2002/66/
[26] E.V. Shuryak, hep-ph/0205031.
[27] U. Heinz and S.M.H. Wong, Phys. Rev. C **66**, 014907 (2002).
[28] B.B. Back *et al.*, PHOBOS Collaboration, nucl-ex/0206012; T. Sakaguchi for the PHENIX Collaboration, nucl-ex/0209030 (to be published in Ref. [1]).
[29] J.-Y. Ollitrault, Phys. Rev. D **46**, 229 (1992).
[30] H. Sorge, Phys. Rev. Lett. **78**, 2309 (1997).
[31] S. A. Voloshin, nucl-ex/0210014 (to be published in Ref. [1]).
[32] A. Dumitru, nucl-th/0206011; D. Teaney, nucl-th/0209024 (to be published in Ref. [1]).
[33] Z. Lin, C.M. Ko, and S. Pal, Phys. Rev. Lett. **89**, 152301 (2002).
[34] S. Soff, S. A. Bass, D. H. Hardtke, and S. Y. Panitkin, nucl-th/0209055 (to be published in Ref. [1]).
[35] R. Rapp, in *Proceedings of 18th Winter Workshop on Nuclear Dynamics, Nassau (Bahamas)*, edited by R. Bellwied, J. Harris, and W. Bauer (EP Systema, Debrecen, 2002); R. Rapp, nucl-th/0204003.